

# The Influence of Inclusions on the Toughness and Fatigue Properties of A516-70 Steel

**A. D. WILSON**

Senior Research Engineer,  
Lukens Steel Company,  
Coatesville, Pa. 19320

*The influence of inclusions on the tensile ductility, upper shelf Charpy-V-notch, dynamic tear and J-integral fracture toughness and the fatigue crack propagation behavior and the fatigue endurance limit of A516-70 normalized, carbon plate steel is reported. Three plates made by conventional steelmaking techniques and 4 plates produced using calcium treatment are examined in thickness from 51 mm (2 in.) to 254 mm (10 in.) in up to 6 different testing orientations per plate. Quantitative image analysis is used to establish correlations between the measured mechanical properties and certain inclusion parameters. Inclusions were found to be detrimental to tensile ductility, upper shelf impact and fracture toughness, and the fatigue endurance limit with predominant effect found to be on the fracture toughness properties. Although inclusions were found to influence adversely the fatigue crack propagation behavior, the effect was not substantial in the steels studied. Quantitative image analysis was used to establish that the fatigue crack propagation behavior and tensile ductility are controlled by the average area of an inclusion on the metallographic cross-section corresponding to the plane of fracture, while the upper shelf toughness properties are controlled by the average length of an inclusion. In general A516-70 was found to be less sensitive to inclusions in both toughness and fatigue crack propagation behavior than A533B Class 1.*

## Introduction

A516 Grade 70 is a carbon plate steel, which is used in a number of pressure vessel applications for moderate and lower temperature service. This 262 MPa (38 ksi) minimum yield strength, 483 MPa (70 ksi) minimum tensile strength is used in general pressure vessel applications in the petrochemical and electric power generation industries in plate thicknesses of 25 - 254 mm (1 - 10 in.). In many of these applications A516-70 is used at the highest quality levels obtainable commercially.

Quality levels of steels are improved through use of various advanced steelmaking techniques [1]. In an aluminum killed steel, such as A516, these techniques involve controlling the types and amount of the indigenous sulfide and oxide nonmetallic inclusions. The effects of these various advanced steelmaking techniques on the inclusions and mechanical properties of plate steels have been reported previously for A533B and A516 steels [1-4]. A516 steels made by two advanced steelmaking techniques were examined in a more comprehensive manner in this study. One group of steels was made by conventional techniques (CON) including controlled sulfur level and vacuum degassing. These are compared to steels that were produced as the CON steels except they were also calcium treated (CaT).

Previous studies have identified that CaT will lead to improved levels and isotropy of tensile ductility, Charpy-V-notch (CVN) and dynamic tear (DT) impact upper shelf toughness in A516

and A533B [1-3]. It has also been demonstrated that there can be a significant improvement in the fracture toughness ( $J_{Ic}$ ,  $K_{Ic}$ ) of a variety of CaT aluminum killed plate steels [5]. In addition, it has been shown that inclusions can have an effect on the level and isotropy of fatigue crack propagation (FCP) behavior in A533B steels [6, 7]. The principal purpose of the investigation reported here was to investigate the influence of inclusions on the fracture toughness and the FCP behavior of A516 steels. In addition the effect of inclusions on the CVN and DT properties and fatigue endurance limit are evaluated. Three CON quality plates and 4 CaT quality plates were examined in thicknesses from 51 - 254 mm (2-10 inches).

## Experimental Procedures

**Description of Test Materials.** The chemistries, thicknesses, and identifications of the 7 production plates of A516-70 that were tested are given in Table 1. The rolling ratios used in making the final plate dimensions are also noted in Table 1. Three of the 51 mm (2 in.) CaT plates were from the same heat of steel and were rolled in 3 different rolling ratios from 2.25:1 to 10:1 to examine effectiveness of the inclusion shape control given by CaT. All of the plates were heat treated by normalizing at 899°C (1650°F) and then air cooling.

The inclusions present in these plates correspond to those normally expected in CON and CaT steels [1, 3]. In CON steels Type II manganese sulfide and galaxies of alumina inclusions are present. Fig. 1 shows the MnS inclusions typical of the 51 mm (2 in.) CON plates. The elongated and pancaked nature of these inclusions due to their plastic behavior at hot rolling tempera-

Contributed by the Materials Division for publication in the JOURNAL OF ENGINEERING MATERIALS AND TECHNOLOGY. Manuscript received by the Materials Division, September 10, 1978.

Table 1 Chemistry

Plate Ident.	Gage mm(in.)	Location	C	S	Mn	P	Cu	Si	Ni	Cr	Mo	V	Al	Ca(ppm)	Rolling Ratio*
CON-1	51 (2)	CL	.24	.015	1.11	.010	.27	.22	.24	.11	.05	.001	.037	0.0	2.8:1
CON-2	51 (2)	CL	.25	.022	1.12	.017	.29	.21	.30	.15	.05	.001	.034	0.0	1.9:1
CON-3	190 (7.5)	QL	.23	.013	.98	.013	.13	.25	.14	.08	.03	.002	.039	5.9	1.5:1
		CL	.24	.013	1.02	.011	.14	.25	.15	.08	.03	.002	.040	2.7	
CaT-1	51 (2)	CL	.23	.002	1.00	.010	.12	.23	.17	.08	.06	.003	.046	41.8	5:1
CaT-2	51 (2)	CL	.23	.003	1.03	.009	.12	.20	.17	.07	.06	.001	.041	46.6	2.3:1
CaT-3	51 (2)	CL	.27	.0014	1.10	.021	.12	.21	.20	.07	.06	.002	.038	28.8	10:1
CaT-4	254 (10)	QL	.24	.002	1.09	.014	.11	.19	.20	.06	.05	.002	.038	42.5	NA
		CL	.25	.002	1.05	.016	.11	.20	.20	.07	.05	.002	.047	41.2	NA

NA = Not available

\* = Ratio of longitudinal to transverse rolling

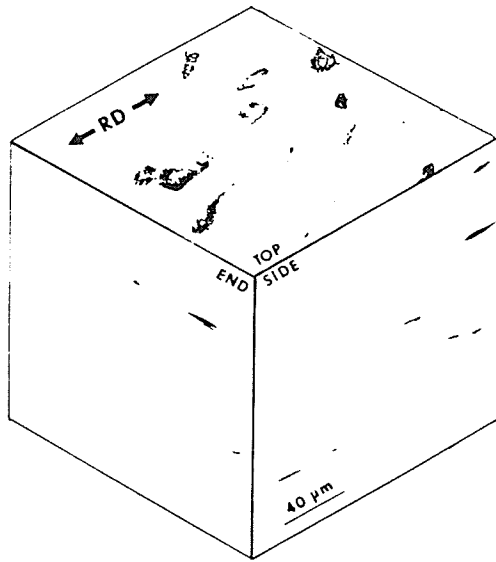


Fig. 1 Composite of light photomicrographs from 51 mm (2 in.) CON-2 steel exhibiting morphology of largest Type II manganese sulfides

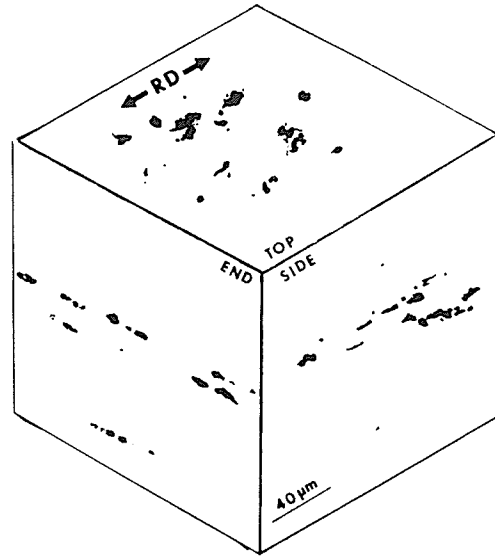


Fig. 2 Composite of light photomicrographs from 51 mm (2 in.) CON-2 steel exhibiting morphology of largest alumina galaxies

tures is evident. The alumina galaxies in the 51 mm (2 in.) CON plates are shown in Fig. 2. Although the individual  $Al_2O_3$  inclusions do not deform on hot rolling, the cluster is rotated and aligned in a planar array. In the thicker 190 mm (7.5 in.) CON-3 plate there was less apparent deformation on the MnS, and less alignment of the  $Al_2O_3$  galaxies, as has been shown previously [3].

In the CaT steels both the Type II MnS and  $Al_2O_3$  galaxies are prevented from forming through desulfurization and inclusion shape control. CaT steels are produced to a 0.010 percent maximum. The amount of desulfurization is evident in Table 1, the sulfur content of the CON steels being 0.013 - 0.022 weight percent, while in these CaT steels it was nominally 0.002 percent. Generally, the inclusions in CaT steels are either the desirable dispersed, compact Type III MnS or duplex and calcium modified, made up of sulfide and aluminate compounds of calcium [1]. Because of the very low sulfur levels of these CaT steels studied here, only the calcium modified inclusions were found. The calcium modification gives inclusion shape control because these inclusions are very hard at hot rolling temperatures and do not elongate. Thus the inclusions in the 51 mm (2 in.) plates (Fig. 3) and the 254 mm (10 in.) plates appear very similar [3]. In addition the inclusions in the 3 CaT plates with 3 different rolling ratios (CaT-1, CaT-2, CaT-3) appeared identical [3].

The microstructures of these A516 steels were as expected, with ferrite and pearlite phases typical for the carbon content of these plates. The major microstructural differences were found to be due to plate thickness and were in the nature of the banded structure. In the thinner plates, the bands of pearlite are much

closer together and a finer ferritic-pearlite structure was generally present.

**Test Locations and Orientations.** All testing of the 51 mm (2 in.) plates was performed on material taken from the plate centerline (CL). The tensile and axial fatigue tests were taken in the longitudinal (L) and transverse (T) orientations. The CVN, DT, FCP, and  $J$ -integral tests were taken in the longitudinal (LT) and transverse (TL) orientations.<sup>1</sup> The drop weight (NDT) tests were taken in the transverse orientation (TS).

Testing of the heavy plates was done at both the CL and quarterline (QL). Tensile tests were taken at both locations in the L, T, and through-thickness (S) orientations. The CVN, DT, and  $J$ -integral tests were taken at the CL in the LT, TL, and through-thickness (SL) orientations. The CVN and FCP tests at the QL were taken in all 6 possible orientations, LS, LT, TS, TL, ST, SL. The drop weight tests to determine the nil-ductility temperature (NDT) were taken at the CL in the transverse orientation (TS). To provide further evidence of the inclusion effect on A516 the fracture surfaces of a number of test specimens were examined in the scanning electron microscope (SEM).

**Basic Mechanical Testing.** The tensile, CVN, DT, and NDT tests were all performed according to the applicable ASTM specifications, namely, E8, E23, E604, and E208[8]. The tensile

<sup>1</sup>According to ASTM E399 [8] the first letter indicates the direction normal to intended crack plane, the second letter indicates the direction of expected crack propagation.

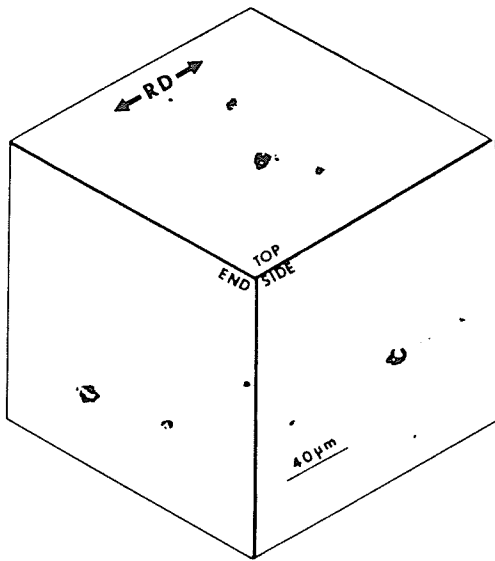


Fig. 3 Composite of light photomicrographs from 51 mm (2 in.) Cat-1 steel displaying morphology of largest calcium modified inclusions

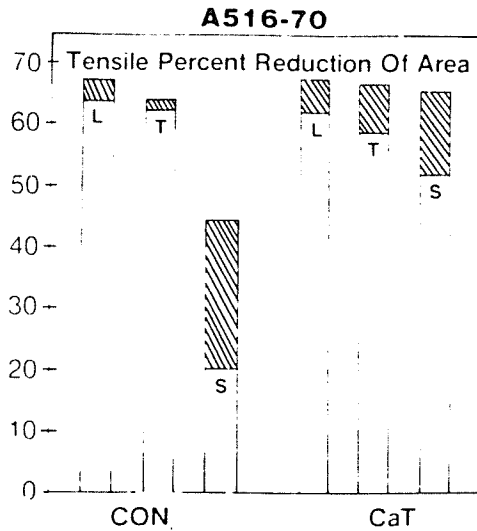


Fig. 4 Level and range (shaded area) of tensile percent reduction of area

properties were obtained at room temperature (R.T.) using two 0.252 in. (6.4 mm) diameter specimens. The full transition curves were obtained in both CVN and DT testing and the respective upper shelf energies were obtained by averaging 3-5 CVN and 2-3 DT results which had 100 percent fracture appearance. The CVN tests used the conventional 0.394 in. (10 mm) square specimen, the DT and NDT tests used 5/8 in. (16 mm) thick specimens.

**J-Integral Testing.** The fracture toughness of the steels was established by determining the  $J_{Ic}$  value of the  $J$ -integral at the point of crack initiation. The  $J_{Ic}$  tests in this study were performed using the single specimen, compliance unload, technique developed by Clarke, et al. [9]. Two specimens were tested for each location and orientation of concern except for the CON-1 material where only one test per orientation was possible. The tests were conducted at +93°C (+200°F), a temperature expected to give fully ductile upper shelf behavior. This temperature also coincided with the upper shelves of the CVN and DT tests. The testing and analysis procedures that were used are reported in detail elsewhere [5].

**Fatigue Crack Propagation Testing.** The FCP tests were performed in air, at room temperature on 25 mm (1 in.) thick speci-

mens. Two tests per orientation and location were conducted. Material CON-3 specimens were the WOL (wedge-opening loading) design, while the remainder of the specimens were of the CT (compact-type) design. The  $K$  calibration used for the WOL design specimens was that reported by Wessel [10]; that used for the CT design specimens was that given in ASTM E399 [8].

The specimens were tested using a sinusoidal waveform on a MTS closed-loop testing machine. The cyclic frequency during most of the test was 10 Hz. When the crack growth rate was approximately  $1.3 \times 10^{-3}$  mm/cycle ( $5 \times 10^{-5}$  in./cycle) the frequency was changed to 1 Hz in order to obtain more data. For both specimen types the load ratio,  $R$  was 0.1. The work of Hudak, et al. [11] in developing a FCP standard test method, which helped lead to ASTM E647 [8] was generally used for guidance in establishing the precracking and testing techniques.

The crack length measurement technique used in this program involved measuring the specimen compliance using a conventional clip gage and determining the crack length during the test through the use of a PDP-8e mini-computer. This procedure has been covered in detail previously [12, 13]. The crack length was calculated from the compliance calibration expressions of Saxena and Hudak [14]. This technique has been demonstrated to give an initial laboratory variability of better than 1.05 in  $da/dN$  [13] which is considerably better than the typical intralaboratory variability of 2.0 reported for the ASTM E24.04 test program using other techniques [15].

In determining the eventual crack growth rate a modified secant method was used, in which the slope between the first and third points of three adjacent crack length - fatigue cycles was used as the crack growth rate for the second point. Plots of  $\log da/dN$  (fatigue crack growth rate) and  $\log \Delta K$  (range of stress intensity factor,  $K_{max} - K_{min}$ ) were then generated and a linear regression then determined the constants  $n$ ,  $C_0$  in the Paris fatigue equation (1) [16].

$$\frac{da}{dN} = C_0(\Delta K)^n \quad (1)$$

$C_0, n = \text{constants}$

**Fatigue Endurance Limit Determination.** Axial fatigue tests were performed on the CON-2 and CaT-3 steels. These 2 steels were chosen for comparison because of their similar yield and tensile strengths. The purpose of the testing was to establish the axial fatigue endurance limit at  $10^7$  cycles in air, at room temperature. The test specimens were 11.1 mm (0.437 in.) diameter with a 44.5 mm (1.75 in.) gage length and a ground surface finish. The specimens were tested in load control at a load ratio of  $R = 0.1$  in an Amsler Vibrophore machine at a frequency of approximately 130 Hz, following ASTM E466 [8]. Eight specimens per orientation were tested to establish stress versus number of cycles to failure (S-N) curves for each material and orientation to establish the fatigue endurance limit at  $10^7$  cycles.

**Quantitative Image Analysis.** Quantitative image analysis (QIA) has been used previously in developing correlations between certain measured inclusion parameters and the tensile ductility, FCP and CVN properties of A533B [1, 2, 7] and the tensile ductility and CVN properties of A516-70 [3]. Three major inclusion parameters have been identified as being important. These are: the area fraction of inclusions ( $A_A$ ), the average area of an inclusion on the plane of fracture ( $\bar{A}$ ), and the average length of an inclusion on the plane and in the direction of fracture ( $\bar{L}$ ) (measured as Feret's diameter). The first parameter  $A_A$  should be the same on all 3 of the major metallographic cross-sections of a plate and is equal to the volume fraction of inclusions, while  $\bar{A}$  can be different for each cross-section and  $\bar{L}$  can vary for each cross-section, as well as vary dependent on the direction of fracture in that cross-section. The techniques that were used in this study to determine the inclusion parameters by QIA have been discussed previously [1, 7].

**Table 2(a) Basic toughness properties**

Ident.	Loc.	Orient.	Charpy-V-Notch	Dynamic Tear	Drop Weight*
			USE J(ft-lb)	USE J(ft-lb)	NDT °C(°F)
CON-1	CL	LT	119 (88)	1010 (745)	-40(-40)
		TL	84 (62)	746 (550)	
CON-2	CL	LT	108 (80)	933 (710)	-40(-40)
		TL	73 (54)	658 (485)	
CON-3	QL	LS	123 (91)	—	—
		LT	119 (88)	—	—
		TS	123 (91)	—	—
		TL	118 (87)	—	—
		ST	66 (49)	—	—
		SL	64 (47)	—	—
	CL	LT	125 (92)	1037 (765)	-40(-40)
		TL	119 (88)	902 (665)	
		SL	69 (51)	556 (410)	

USE - Upper Shelf Energy  
 NDT - Nil-ductility Temperature

\*Tests in TS orientation

**Table 2(b) Basic toughness properties**

Ident.	Loc.	Orient.	Charpy-V-Notch	Dynamic Tear	Drop Weight*
			USE J(ft-lb)	USE J(ft-lb)	NDT °C(°F)
CaT-1	CL	LT	193 (142)	1526 (1125)	-34(-30)
		TL	174 (128)	1302 (960)	
CaT-2	CL	LT	188 (139)	1390 (1025)	-40(-40)
		TL	188 (139)	1417 (1045)	
CaT-3	CL	LT	176 (130)	1553 (1145)	-34(-30)
		TL	156 (115)	1315 (970)	
CaT-4	QL	LS	165 (122)	—	—
		LT	172 (127)	—	—
		TS	153 (113)	—	—
		TL	160 (118)	—	—
		ST	126 (93)	—	—
		SL	122 (90)	—	—
	CL	LT	146 (108)	1227 (905)	-34(-30)
TL		133 (98)	997 (735)		
SL		103 (76)	719 (530)		

\*Tests in TS orientation

USE - Upper Shelf Energy  
 NDT - Nil-ductility Temperature

**Table 3 Fracture toughness results at +93°C(+200°F)**

Plate Identi- fication	Orient.	$(J_{Ic})_g$		$(J_{Ic})_{FLD}$		$(K_{Ic})_g$		$(K_{Ic})_{FLD}$		$(K_{Ic})_{RNB}$		$T$
		$\frac{KJ}{m^2}$	$\frac{(in-lb)}{in^2}$	$\frac{KJ}{m^2}$	$\frac{(in-lb)}{in^2}$	$MPa\sqrt{m}(ksi\sqrt{in})$	$MPa\sqrt{m}(ksi\sqrt{in})$	$MPa\sqrt{m}(ksi\sqrt{in})$	$MPa\sqrt{m}(ksi\sqrt{in})$	$MPa\sqrt{m}(ksi\sqrt{in})$		
CON-1	LT	203 (1160)		295 (1684)		206(187)		247(225)		156(142)		254
	TL	113 (648)*		190 (1084)*		153(139)*		198(180)*		130(118)		177
CON-2	LT	212 (1213)		308 (1759)		210(191)		363(330)		142(129)		303
	TL	104 (593)*		159 (908)*		147(134)*		192(175)*		119(108)		189
CON-3	LT	215 (1230)		338 (1928)		211(192)		264(240)		138(126)		347
	TL	259 (1480)		311 (1774)		232(211)		254(231)		130(118)		308
	SL	149 (848)		167 (954)		176(160)		186(169)		99(90)		185
CaT-1	LT	465 (2655)		578 (3303)		311(283)		346(315)		209(190)		425
	TL	363 (2070)		490 (2800)		275(250)		319(290)		191(174)		327
CaT-2	LT	458 (2613)		556 (3174)		308(280)		340(309)		201(183)		446
	TL	389 (2220)		502 (2864)		284(258)		322(293)		192(175)		431
CaT-3	LT	497 (2840)		584 (3333)		321(292)		237(316)		188(171)		472
	TL	401 (2290)		494 (2821)		288(262)		320(291)		175(159)		442
CaT-4	LT	426 (2435)		392 (2241)		297(270)		285(259)		160(146)		308
	TL	231 (1320)		334 (1908)		219(199)		264(240)		146(133)		306
	SL	255 (1455)		336 (1919)		231(210)		264(240)		129(117)		282

\*Valid Data according to reference [19]

## Results and Discussion<sup>2</sup>

**Basic Mechanical Testing.** The 0.2 percent yield strengths of the steels ranged from 241 - 359 MPa (35 - 52 ksi) and the ultimate tensile strengths varied between 496 - 600 MPa (72 - 87 ksi). The percent elongation values ranged from 7.3 - 33.8 percent. The major difference between the CON and CaT steels was best demonstrated in the values of the percent reduction of area (percent RA), as exhibited in Fig. 4. The primary improvement exhibited by CaT was in the S orientation.

The CVN, DT, and NDT results are summarized in Tables 2(a) and 2(b). The primary improvement demonstrated by the CaT over the CON steels is in the CVN and DT USE's. The level of USE in all testing orientations, particularly in the TL and SL orientation, is higher in the CaT steels. There also is a general improvement in the isotropy exhibited by the CaT steels. A similar improvement is to be expected in both the CVN and DT USE's, since a statistical correlation between them has been established [18].

**$J_{Ic}$  Results.** In this investigation the critical value of  $J$  was determined by two methods, namely, that  $J_{Ic}$  determined using the graphical analysis technique ( $J_{Ic}$ )<sub>G</sub>, [19] and that determined at the point of first load drop from the load-displacement curve, ( $J_{Ic}$ )<sub>FLD</sub> [9]. In the graphical analysis method the ( $J_{Ic}$ )<sub>G</sub> was taken at the intersection of the "blunting line" and the visually determined best fit line through points having the required amount of crack extension according to [19]. The ( $J_{Ic}$ )<sub>FLD</sub> was established at the point of maximum load, since all of the load-displacement curves were smooth with no discontinuities. These determinations are given in Table 3. Those ( $J_{Ic}$ )<sub>G</sub> values that meet the suggested validity requirements [19] including that for specimen size are noted. The specimen size requirement demands that:

$$B, b \geq 25 J/FS \quad (2)$$

Where  $B$  is the specimen thickness,  $b$  is the initial remaining ligament length of the specimen and FS is the flow stress  $\{FS = (0.2YS + UTS)/2\}$ . Those ( $J_{Ic}$ )<sub>FLD</sub> points which would also meet this specimen size requirement are also noted in Table 3. All of the specimen tests which did not meet the validity of specimen size requirements failed due to the remaining ligament length,  $b$ , being undersized.

In addition, in Table 3 the values of  $K_{Ic}$  were established from the following:

$$J_{Ic} = \frac{1 - \nu^2}{E} K_{Ic}^2 \quad (3)$$

The value of  $\nu$  was taken as 0.3 and of  $E$  of 207,000 MPa ( $30 \times 10^6$  psi). Furthermore the Rolfe-Novak-Barson (RNB) upper shelf  $K_{Ic}$  - CVN correlation [20, 21] was used to determine an additional  $K_{Ic}$  value using the CVN USE values of Tables 2(a) and 2(b). This correlation is:

$$\left( \frac{K_{Ic}}{0.2YS} \right)^2 = 5 \left( \frac{CVN \text{ USE}}{0.2YS} - 0.05 \right) \quad (4)$$

where 0.2YS is in ksi, CVN USE in ft-lb and  $K_{Ic}$  is  $\text{ksi}\sqrt{\text{in}}$ . Also given in Table 3 is the value of  $T$ , the tearing modulus, developed by Paris, et al. [22].  $T$  is calculated from the following:

$$T = \frac{dJ}{da} \frac{E}{(FS)^2} \quad (5)$$

where  $dJ/da$  was taken as the slope of the best fit straight line from the  $J - \Delta a$  R-curve used in determining the previous ( $J_{Ic}$ )<sub>G</sub> value. The higher the  $T$  value the higher the resistance of

the material to continued slow stable crack growth after the  $J_{Ic}$  point (crack initiation) has occurred.

$J_{Ic}$  results once more demonstrate the improved level of toughness and isotropy present in the CaT steels. It has been reported previously [5] that the  $J_{Ic}$  test tends to be more sensitive to inclusion differences than the CVN and DT tests and it generally appears to be the case for the A516 data reported here. Whether the ( $J_{Ic}$ )<sub>G</sub> or ( $J_{Ic}$ )<sub>FLD</sub> gives the more reliable result for A516 is difficult to establish since most of the data are invalid due to the undersized specimens. It does appear, however, that the ( $J_{Ic}$ )<sub>FLD</sub> results tend to be more consistent, although they also tend to indicate higher toughness as well.

The  $K_{Ic}$  values also indicate the improved quality of the CaT steels, however it can be noted that the  $K_{Ic}$  values determined from  $J_{Ic}$  are significantly higher than those obtained from the RNB correlation. This is not surprising since the RNB correlation is intended for higher strength steels with little or no loading rate sensitivity. It would be expected that the A516 steels would be very sensitive to loading rate and thus a static property,  $K_{Ic}$ , couldn't be reliably calculated from the dynamic CVN data, while also using static tensile properties.

It also should be noted that most of the  $J_{Ic}$ ,  $K_{Ic}$  values reported are invalid results because of the low strength and high toughness generally exhibited by A516. To obtain plane strain conditions with the lowest toughness reported here,  $153 \text{ MPa}\sqrt{\text{in}}$  ( $139 \text{ ksi}\sqrt{\text{in}}$ ) and the highest strength level,  $376 \text{ MPa}$  ( $54.6 \text{ ksi}$ ) would require a structural application thickness of 390 mm (16 in.). Therefore, in most applications it would be expected that designing using  $K_{Ic}$  would be very conservative, i.e., there would be slow stable crack growth after crack initiation prior to instability and final failure. This particular area of research has been very active recently in trying to identify a parameter or parameters that best quantify the slow stable growth of a ductile crack [23]. The parameter  $T$  has been mentioned as having possible application in this area and thus the higher  $T$  values shown in Table 3 for the CaT steels are further evidence of the increased fracture toughness displayed by these steels.

Scatterbands encompassing all of the  $J$  versus  $\Delta a$  R-curves in this investigation are given in Fig. 5. From this figure it can generally be noted that the CaT steel R-curves are shifted to higher toughnesses ( $J$  values) with steeper slopes ( $T$  values).

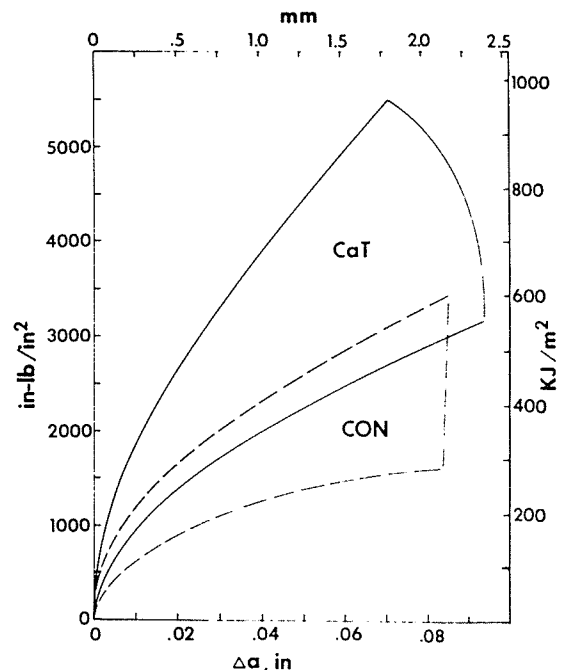
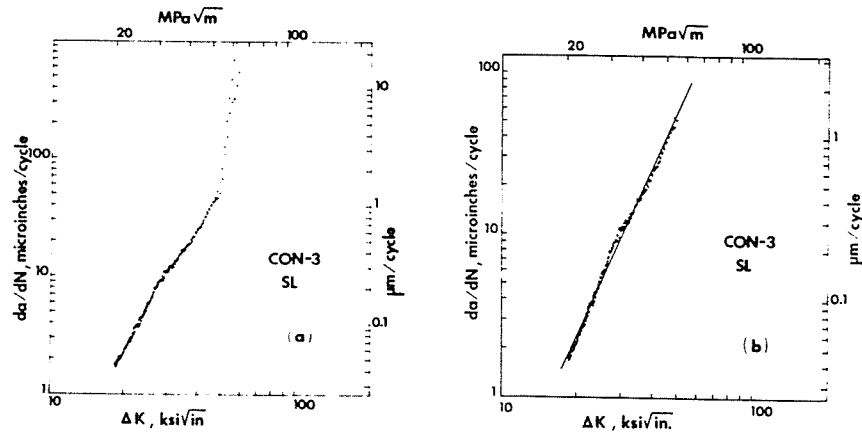


Fig. 5 Scatter bands for all  $J$  versus crack extension ( $\Delta a$ ) resistance curves

<sup>2</sup>A more detailed presentation of the results of this testing program may be found in [17].



**Fig. 6 Data plots of 2 tests for CON-3 steel in SL orientation of fatigue crack growth rate versus range of stress intensity factor. (a) All data. (b) Data with  $da/dN$  greater than  $1.5 \times 10^{-3}$  mm/cycle ( $6 \times 10^{-5}$  in./cycle) has been eliminated and best fit regression line for data determined.**

**Fatigue Crack Propagation.** All of the FCP data was initially plotted in  $\Delta K - da/dN$  curves. An example is shown in Fig. 6(a). The upswing of the data at the higher  $\Delta K - da/dN$  levels is due to the large amount of plastic deformation developing in this low strength, high toughness steel at long crack lengths. Therefore, the data in this area of the curve should not be included in the analysis and comparison. It was found that the upswing in the FCP data would be eliminated for all of the FCP tests by restricting the regression analyses to data with a  $da/dN$  of less than  $1.5 \times 10^{-3}$  mm/cycle ( $6 \times 10^{-5}$  in./cycle). This resulted in the curve shown in Fig. 6(b) for the same data shown in Fig. 6(a). These data were then used in determining the best fit straight line by regression analysis and thus determining the FCP constants in the Paris equation (1). The slight "knee" in the data shown in Fig. 6(b) at a  $\Delta K$  of  $33 \text{ MPa}\sqrt{\text{in.}}$  ( $30 \text{ ksi}\sqrt{\text{in.}}$ ) was present in all of the test results.

The results of all of the FCP tests are given in Table 5 in the form of the FCP constants  $n$  and  $C_0$ . Also, the statistical parameter  $R^2$  is given. A value for  $R^2$  of 1.0 would signify a perfect fit of the regression line to the data. All of the  $R^2$  values are at 0.98 or better with most at 0.99 or better, indicating the excellent

agreement between the regression analysis line (and thus the  $n$  and  $C_0$  values) and the test data. The excellent statistical fit of the data allows for confident and definitive comparisons between steels and testing orientations.

In general in this study of A516 the differences in FCP behavior between and within steels of different inclusion structures were found to be less dramatic than those found previously in A533B [6]. In that study of A533B steels of 3 levels of inclusion structure, for example, the range in  $n$  values was from 2.39 to 3.74. In the A516 steels, however, consistent, though small, differences were detected which can be attributed to inclusion structure.

In the CON-3 steel the  $n$  values for the through-thickness testing orientations, ST and SL were higher than in the other orientations. This is the first indication of anisotropy of FCP in this steel. In contrast, the CaT-4 steel ST and SL  $n$  values are more in line with those in the other orientations. Fig. 7 additionally shows the improved level and isotropy of CaT-4 on the through-thickness direction. This figure and the FCP constants in Table 4 for the two materials, indicate that the CON-3 steel generally exhibits slightly faster fatigue crack growth rates than the CaT-4 steel at higher  $\Delta K$  levels, in the ST and SL orientations. How-

**Table 4 Fatigue crack propagation results**

Plate Identification			$C_0^*$		$n$	$R^2$
			MPa $\sqrt{\text{m}}$ , mm/cycle)	(ksi $\sqrt{\text{in.}}$ , in./cycle)		
CON-1	CL	LT	$1.069 \times 10^{-8}$	$(5.508 \times 10^{-10})$	2.851	.9953
		TL	$4.467 \times 10^{-9}$	$(2.355 \times 10^{-10})$	3.099	.9941
CON-2	CL	LT	$6.516 \times 10^{-9}$	$(3.404 \times 10^{-10})$	2.991	.9902
		TL	$4.539 \times 10^{-9}$	$(2.399 \times 10^{-10})$	3.112	.9922
CON-3	QL	LS	$2.979 \times 10^{-9}$	$(1.581 \times 10^{-10})$	3.187	.9888
		LT	$3.475 \times 10^{-9}$	$(1.845 \times 10^{-10})$	3.166	.9923
		TS	$2.606 \times 10^{-9}$	$(1.390 \times 10^{-10})$	3.225	.9844
		TL	$3.112 \times 10^{-9}$	$(1.660 \times 10^{-10})$	3.202	.9949
		ST	$1.079 \times 10^{-9}$	$(5.929 \times 10^{-11})$	3.538	.9879
		SL	$1.315 \times 10^{-9}$	$(7.194 \times 10^{-11})$	3.481	.9922
CaT-1	CL	LT	$8.974 \times 10^{-9}$	$(4.634 \times 10^{-10})$	2.878	.9941
		TL	$6.486 \times 10^{-9}$	$(3.381 \times 10^{-10})$	2.963	.9833
CaT-2	CL	LT	$9.441 \times 10^{-9}$	$(4.875 \times 10^{-10})$	2.871	.9956
		TL	$3.459 \times 10^{-9}$	$(1.854 \times 10^{-10})$	3.150	.9923
CaT-3	CL	LT	$6.281 \times 10^{-9}$	$(3.273 \times 10^{-10})$	2.970	.9926
		TL	$3.767 \times 10^{-9}$	$(1.991 \times 10^{-10})$	3.110	.9924
CaT-4	QL	LS	$5.200 \times 10^{-9}$	$(2.729 \times 10^{-10})$	3.027	.9906
		LT	$5.623 \times 10^{-9}$	$(2.944 \times 10^{-10})$	3.032	.9906
		TS	$4.560 \times 10^{-9}$	$(2.399 \times 10^{-10})$	3.066	.9856
		TL	$5.821 \times 10^{-9}$	$(3.048 \times 10^{-10})$	3.020	.9938
		ST	$3.443 \times 10^{-9}$	$(1.832 \times 10^{-10})$	3.180	.9868
		SL	$3.006 \times 10^{-9}$	$(1.607 \times 10^{-10})$	3.229	.9891

\*Determined when  $\Delta K$  and  $da/dN$  had the dimensions indicated below.

Table 5 FCP constants summary

		$C_0^*$		n	$R^2$
		MPa $\sqrt{m}$ , mm/cy	ksi $\sqrt{in.}$ , in/cy		
51 mm (2 in.) Steels					
CON	LT	$8.492 \times 10^{-9}$	$4.406 \times 10^{-10}$	2.916	.9922
	TL	$4.560 \times 10^{-9}$	$2.404 \times 10^{-10}$	3.102	.9922
CaT	LT	$8.091 \times 10^{-9}$	$4.188 \times 10^{-10}$	2.907	.9933
	TL	$4.365 \times 10^{-9}$	$2.296 \times 10^{-10}$	3.076	.9891
All	LT	$8.610 \times 10^{-9}$	$4.457 \times 10^{-10}$	2.899	.9912
All	TL	$4.487 \times 10^{-9}$	$2.366 \times 10^{-10}$	3.083	.9863
All Data		$6.067 \times 10^{-9}$	$3.170 \times 10^{-10}$	2.997	.9875
Thick Steels					
All	LT	$4.375 \times 10^{-9}$	$2.307 \times 10^{-10}$	3.101	.9910
All	TL	$4.742 \times 10^{-9}$	$2.495 \times 10^{-10}$	3.079	.9934
all LT and TL		$4.519 \times 10^{-9}$	$2.382 \times 10^{-10}$	3.092	.9920
All Steels in This Study		$4.581 \times 10^{-9}$	$2.410 \times 10^{-10}$	3.083	.9837

\*Determined when  $\Delta K$  and  $da/dN$  had the dimensions indicated below.

ever, it is only in these through-thickness orientations in which any significant difference is noted. As is displayed in the summary scatterbands for the heavy gage materials in Fig. 8 and for the light gage steels in Fig. 9, there is no substantial difference in the FCP behavior between the CaT and CON steels. This is further demonstrated in the calculated summaries given in Table 5. Table 5 in addition indicates that there is no significant difference between the light and heavy gage plates in this study. It therefore appears that extensive hot working in one direction with much higher inclusion content is necessary in carbon steels before there is a substantial effect on the FCP growth rate [24, 25].

**Fatigue Endurance Limit.** The results of the axial fatigue tests are given in Fig. 10. No significant difference between the L and T orientations were found for either the CON-2 or CaT-3 steels, therefore the best fit straight lines for each steel used both the

L and T data. The apparent fatigue endurance limit at 10<sup>7</sup> cycles of the CON-2 steel was 345 MPa (50 ksi), while for the CaT-3 steel it was 379 MPa (55 ksi). This improvement of the CaT steel over the CON steel in the "high-cycle fatigue" area would appear to be related to the lower inclusion content and smaller inclusion sizes in the CaT steels.

**Inclusion Correlations.** Plots of the inclusion parameters versus the various toughness and FCP parameters that have been determined in this study were made to establish whether any correlations existed. No correlations were established with the fatigue endurance limit results because of the limited axial fatigue testing that was done. After identifying the likely candidates for correlations between a specific inclusion parameter and a particular mechanical property, linear regression analysis was used to obtain the regression equation and to establish if a significant statistical correlation existed. Table 6 lists all those correlations that were found with a statistical significance level of 99 percent or greater. Also Fig. 11 shows the data plots of the best correlations that were established.

The results in Table 6 reveal that the FCP parameters  $n$  and  $\log C_0$ , as well as the percent RA correlate best with the inclusion

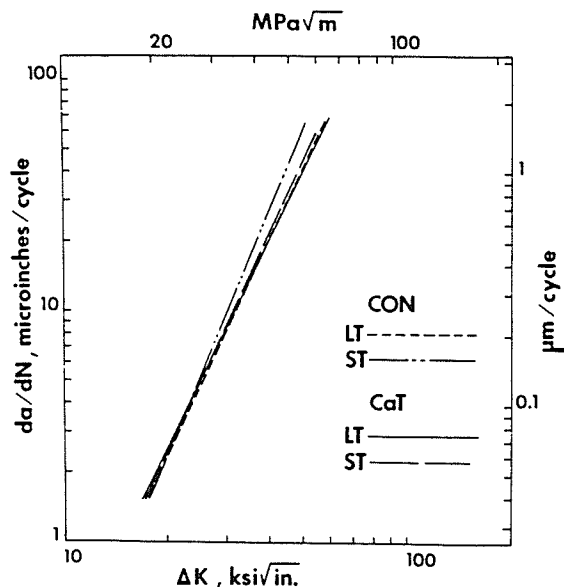


Fig. 7 Plots of fatigue crack growth rate versus range of stress intensity factor comparing the CON-3 and CaT-4 steels in LT and ST orientations

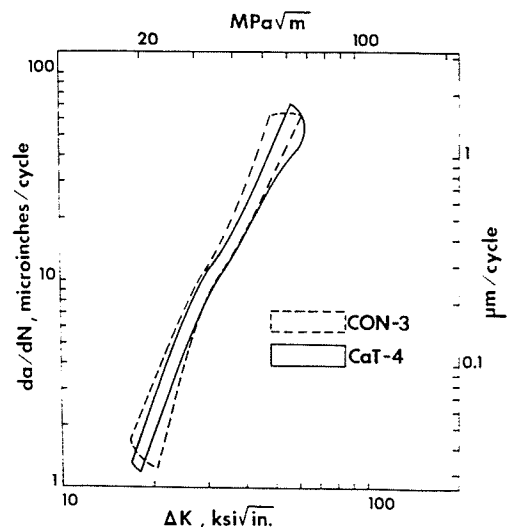


Fig. 8 Summary scatterbands of fatigue crack growth rate versus range of stress intensity factor comparing all data for CON-3 and CaT-4 thick gage steels

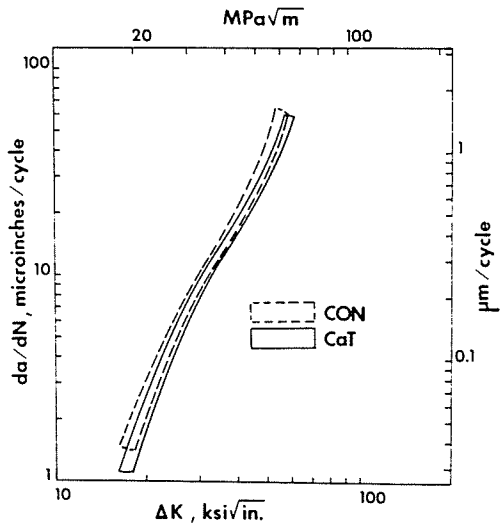


Fig. 9 Summary scatterbands of fatigue crack growth rate versus range of stress intensity factor comparing all data for 51 mm (2 in.) CON and CaT steels

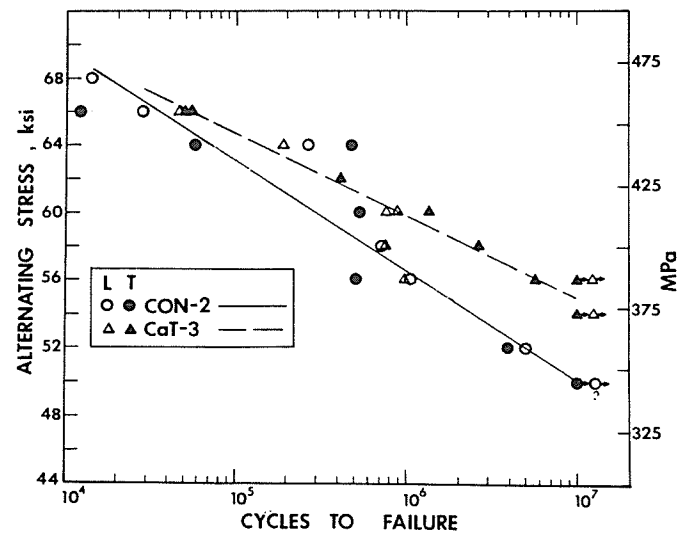


Fig. 10 Plot of axial fatigue data, alternating stress versus number of cycles to failure for CON-2 and CaT-3 steels

parameter  $\bar{A}$ . On the other hand, the toughness measurements  $T$ ,  $J_{Ic}$ ,  $K_{Ic}$ , CVN USE, and DT USE, correlate best with  $\bar{L}$ . No significant correlations were found between  $A_A$  and any of these mechanical properties. In all cases the regression equations that were determined indicate that inclusions are detrimental to ductility, toughness and FCP behavior.

The above observations establish that the parameter  $\bar{A}$  provides the best correlation with the FCP parameters and the percent RA. Both of these properties are generally not appreciably affected by moderate changes in inclusion structure. For example, the longitudinal and transverse oriented tests for both properties do not change significantly with inclusion structure, while the most significant changes are often found in the through-thickness orientations. This also corresponds to the behavior of the  $\bar{A}$  parameter, which is largest for the through-thickness tests of CON steels, and not as significantly affected by steelmaking

practice in the other orientations. This is due to the pancaking effect of rolling on the Type II MnS inclusions in CON steels as shown in the Top cross-section of Fig. 1. The  $\bar{A}$  parameter tends to indicate the presence of these large inclusion surfaces which can act as planes of weakness in a steel. CaT prevents the formation of these large inclusion surfaces through both desulfurization and inclusion shape control and thus results in the improved FCP and percent RA properties for CaT steels in the through-thickness testing orientations.

The toughness properties were found to correlate best with the  $\bar{L}$  parameter. The toughness properties were also found to be much more sensitive to inclusion structure than the FCP parameters or the percent RA. Changes in inclusion structure generally can have a significant effect on the toughness properties in any of the three major testing orientations. The  $\bar{L}$  parameter is also similarly affected in that steelmaking practice can significantly

Table 6 Inclusion correlations\*

$n$	=	$2.728 + 0.007689\bar{A}$	.6703
$\log C_o^+$ (MPa√m, mm/cy)	=	$-7.842 - 0.01079\bar{A}$	
(ksi√in., in/cy)	=	$-9.135 - 0.01047\bar{A}$	.6498
$T$	=	$552.5 - 25.14\bar{L}$	.3984
$(J_{Ic})_G$ (KJ/m <sup>2</sup> )	=	$637.8 - 37.76\bar{L}$	
(in.-lb/in. <sup>2</sup> )	=	$3.642 \times 10^3 - 215.6\bar{L}$	.4880
$(J_{Ic})_{FLD}$ (KJ/m <sup>2</sup> )	=	$789.0 - 45.53\bar{L}$	
(in.-lb/in. <sup>2</sup> )	=	$4.505 \times 10^3 - 260.0\bar{L}$	.5994
$(K_{Ic})_G$ (MPa√m)	=	$387.8 - 16.17\bar{L}$	
(ksi√in.)	=	$352.9 - 14.71\bar{L}$	.4742
$(K_{Ic})_{FLD}$ (MPa√m)	=	$442.2 - 17.75\bar{L}$	
(ksi√in.)	=	$402.4 - 16.15\bar{L}$	.5556
% RA	=	$78.55 - 0.3314\bar{A}$	.5887
% RA	=	$78.52 - 2.288\bar{L}$	.2176
CVN USE (J)	=	$180.6 - 0.8674\bar{A}$	
(ft-lb)	=	$133.2 - 0.6397\bar{A}$	.2131
CVN USE (J)	=	$223.3 - 10.81\bar{L}$	
(ft-lb)	=	$164.7 - 7.974\bar{L}$	.4518
DT USE (J)	=	$2042 - 106.2\bar{L}$	
(ft-lb)	=	$1506 - 78.31\bar{L}$	.6578

\* $A_A$  - Area Fraction, Percent

$\bar{A}$  - Average Area,  $\mu\text{m}^2$

$\bar{L}$  - Average Length,  $\mu\text{m}$

At 99 percent Significance Level or Greater.

+ Determined when  $\Delta K$  and  $da/dN$  had the dimensions indicated.

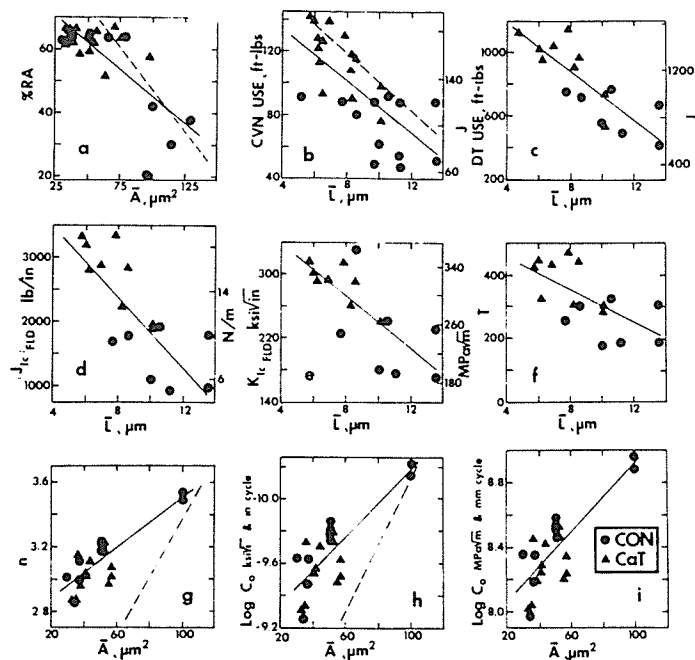


Fig. 11 Plots of various mechanical properties versus inclusion parameters. Regression line indicated as solid line. Dashed line represents A533B data determined in [2 and 7]. In Figs. (h) and (i)  $C_0$  values determined when  $\Delta K$  and  $da/dN$  had dimensions indicated.

change  $\bar{L}$  in all cross-sections. The  $\bar{L}$  parameter indicates the presence of long inclusions. This primarily is related to the elongation of the Type II MnS inclusions on hot rolling of the steel plate. CaT limits the presence of long inclusions via desulfurization and inclusion shape control and thus leads to the improved toughness properties in these steels in all testing orientations.

The correlation with different inclusion parameters of the mechanical properties discussed above may be due to a number of causes. For example, the toughness tests look at the steel under a very large plastic zone at the crack tip compared to that acting in a FCP test. Therefore the toughness tests view a much larger volume of material and thus have a greater opportunity to find inclusions to initiate and propagate fracture. Thus the toughness tests are more sensitive to changes in inclusion structure. Apparently this sensitivity is caused by the presence of long inclusions. Another cause of the different correlations may be due to the FCP and tensile ductility tests being performed under conditions of more constraint or triaxiality, compared to the extensive plastic deformation exhibited in the toughness tests, particularly in the CaT steels.

An additional item to note in the inclusion equations in Table 7 is that the  $(J_{IC})_{FLD}$  and  $(K_{IC})_{FLD}$  values gave better correlations with the  $\bar{L}$  inclusion parameter than did the  $(J_{IC})_G$  and  $(K_{IC})_G$  values. Remembering that the majority of these fracture toughness data determined using the  $J$ -integral were invalid, this may indicate that when using invalid data the FLD results are the more reliable for comparing steel toughness levels.

Also given in Fig. 11 are the inclusion correlations previously determined for A533B Class 1 [2, 7]. These lines in the FCP, percent RA, and CVN USE graphs demonstrate what we have discussed in previous sections. That is, the A516 steel is not as sensitive to inclusion structure as A533B Class 1, particularly in properties that correlate best with  $\bar{A}$ . The primary difference between these two steels is that A533B is a quenched and tempered, bainitic low alloy steel, while A516 is a normalized, ferritic-pearlitic carbon steel. A 533B also is a stronger steel with a 345 MPa (50 ksi) minimum yield strength. Whether the above differences between A533B and A516 are due to the metallurgical constituents or the strength level cannot be definitely established

at this time. However, it is suggested that the strength level is the primary cause, due to its direct effect on the plastic zone size operating at the crack tip and thus on the resulting inclusion interaction.

The above discussion has been based primarily on the QIA developed inclusion correlations. Unfortunately QIA is not infallible and also will not quantify the group nature in which the Type II MnS and  $Al_2O_3$  galaxies in CON steel act. In addition the presence of large clusters of small alumina inclusions will tend to average out the large, elongated MnS inclusions in the QIA of CON steels, thus making subtle differences difficult to detect. On the whole, however, the presence of large inclusions and inclusion surfaces have been detected. This is demonstrated by the results as plotted in Fig. 11 and the 99 percent significance level of the statistical analyses in Table 6.

**Fractography.** Fractographic examination of mechanical testing specimen fractures has been found to be an invaluable aid in identifying the kinds of inclusions present in a steel and in explaining the influence of inclusions on mechanical properties [1, 7, 26]. The fractographic examinations made in this study used the scanning electron microscope (SEM). In general no significant differences were found between these investigations and previous ones on A533B steel [1, 7, 26].<sup>3</sup>

## Conclusions

It has been generally found in this investigation that inclusions have a considerable detrimental effect on the toughness properties of A516-70, while they have a small and consistent but not substantial effect on the FCP properties. The difference in the interaction of inclusions with toughness and in FCP behavior is further pointed out in the inclusion correlations. The FCP parameters correlate best with  $\bar{A}$ , a measure of the presence of large inclusions surfaces, while the toughness properties correlate best with  $\bar{L}$ , a measure of the presence of large inclusions lengths. These differences appear to be due to the size of the plastic zone controlling each of these tests and the interaction of the particular crack front with the inclusion groups present in the CON steels. Furthermore, it has been found that this lower strength A516-70 steel is less sensitive to inclusions than the previously examined higher strength A533B Class 1 steel [2, 7]. The FCP growth rates for A516 also appear substantially unaffected by the plate thickness from which samples are taken. In addition the fatigue endurance limit is slightly improved in CaT steels.

It has been reported that inclusions can increase the FCP growth rate in aluminum alloys [27-29] and steels [24, 25, 30], lead to retardation in aluminum alloys [31] or steels [32], and either retard or accelerate the FCP growth rate dependent on the  $\Delta K$  level in aluminum alloys [33] or steels [6]. The work presented here suggests that there is an additional variable contributing to the interaction of inclusions with FCP behavior that should be considered, i.e., the material strength properties. Further work in this area appears warranted.

FCP parameters determined in this study are very close to those reported previously for a number of ferritic-pearlitic steels by Barsom [34] and for A516-60 by Crooker and Sullivan [35]. This is a further indication of the apparent slight sensitivity of FCP in low strength carbon steels to moderate metallurgical differences that may occur within specifications ranges.

## Acknowledgments

The author wishes to acknowledge the contributions of J. K. Donald and D. W. Schmidt of the Del Research Division of the Philadelphia Suburban Corporation for performing the single specimen  $J$ -integral and fatigue crack propagation tests. The efforts of L. K. Kerr in performing the other mechanical tests is

<sup>3</sup>A summary of the fractographic results of this and previous investigations [1, 7] will be the subject of a future publication.

also appreciated, as is the assistance of T. R. Stetler in the statistical analyses and J. R. Lohr for metallographic assistance. The QIA work was performed by Structure Probe Inc. and the SEM studies done at SKF Industries, Inc. D. A. Boe is thanked for providing some of the conventional mechanical data.

The guidance and comments provided by J. A. Gulya during the experimental and writing aspects of this research are also appreciatively acknowledged.

## Disclaimer

It is understood that the material in this paper is intended for general information only and should not be used in relation to any specific application without independent examination and verification of its applicability and suitability by professionally qualified personnel. Those making use thereof or relying thereon assume all risk and liability arising from such use or reliance.

## References

- 1 Wilson, A. D., "The Effect of Advanced Steelmaking Techniques on the Inclusions and Mechanical Properties of Plate Steels," presented at AIME Annual Meeting, Atlanta, GA, March 1977, to be published.
- 2 Wilson, A. D., "The Interaction of Advanced Steelmaking Techniques, Inclusions, Toughness and Ductility in A533B Steels," ASM, Technical Report System No. 76-02, 1976.
- 3 Wilson, A. D., "The Influence of Thickness and Rolling Ratio on the Inclusion Behavior in Plate Steels," presented at ASM Materials Conference, Chicago, Ill., Oct. 1977, accepted for publication in *Metallography*.
- 4 Elwell, R. H., Strattan, J. K., and Swift, R. A., "The Improvements in the Mechanical Properties of Heavy Gauge A516-70 Carbon Steel," *Effects of Melting and Processing Variables on the Mechanical Properties of Steel*, ed. Smith, G. V., ASME, N. Y., 1977, pp. 41-59.
- 5 Wilson, A. D., "The Characterization of Plate Steel Quality Using Various Toughness Measurement Techniques," in *Elastic-Plastic Fracture*, ASTM STP 668, ASTM, 1979, pp. 469-492.
- 6 Wilson, A. D., "Fatigue Crack Propagation in A533B Steels," *ASME Journal of Pressure Vessel Technology*, Vol. 99, No. 3, Aug. 1977, pp. 459-469.
- 7 Wilson, A. D., "Fatigue Crack Propagation in A533B Steels - Metallographic and Fractographic Analyses," *ASME Journal of Pressure Vessel Technology*, Vol. 101, No. 2, May 1979, pp. 155-164.
- 8 1978 *Annual Book of ASTM Standards, Part 10*, ASTM, Philadelphia, pp. 512-533, pp. 160-180, pp. 235-251, pp. 617-625, pp. 364-383, pp. 662-680, pp. 546-551.
- 9 Clarke, G. A., Andrews, W. R., Paris, P. C., and Schmidt, D. W., "Single Specimen Tests for  $J_{Ic}$  Determination" in *Mechanics of Crack Growth*, ASTM STP 590, ASTM, 1976, pp. 27-42.
- 10 Wessel, E. T., "State of the Art of the WOL Specimen for  $K_{Ic}$  Fracture Toughness Testing," *Engineering Fracture Mechanics*, Vol. 1, No. 1, June 1968, p. 77.
- 11 Hudak, S. J., Jr., Saxena, A., Bucci, R. J., and Malcolm, R. C., "Development of Standard Methods of Testing and Analyzing Fatigue Crack Growth Rate Data (Third Semi-Annual Report)," AFML Contract F33615-75-C-5064, Project FY-1457-75-02110/7381, Mar. 10, 1977.
- 12 Saxena, A., Hudak, S. J., Jr., Donald, J. K., and Schmidt, D. W., "Computer Controlled K-Decreasing Technique for Low-Rate Fatigue Crack Growth Testing," *ASTM, Journal of Testing and Evaluation*, Vol. 6, No. 3, May 1978, pp. 167-174.
- 13 Donald, J. K., and Schmidt, D. W., "Computer Controlled K-Gradient Technique for High-Growth Rate Fatigue Crack Growth Testing," presented ASTM E24.04 Committee Meeting, November 9, 1978, Philadelphia.
- 14 Saxena, A., and Hudak, Jr., S. J., "Review and Extension of Compliance Information for Common Crack Growth Specimens," Westinghouse Scientific Paper 77-9E7-AFCGR-P1, May 3, 1977.
- 15 Clark, W. G., Jr., and Hudak, S. J., Jr., "Variability in Fatigue Crack Growth Rate Testing," *ASTM, Journal of Testing and Evaluation*, Vol. 3, No. 6, pp. 454-476.
- 16 Paris, P. C., "Fatigue, and Interdisciplinary Approach," Sagamore, New York, 1964, p. 107.
- 17 Wilson, A. D., "The Influence of Inclusions on the Toughness and Fatigue Properties of A516-70 Steel," Lukens Steel Research Report RDR 78-6, August 1978.
- 18 Wilson, A. D., "Comparison of Dynamic Tear and Charpy-V-Notch Impact Properties of Plate Steels," *ASME JOURNAL OF ENGINEERING MATERIALS AND TECHNOLOGY*, Vol. 100, No. 2, Apr. 1978, pp. 204-211.
- 19 Clarke, G. A., "Recommended Procedure for  $J_{Ic}$  Determination," presented at the ASTM E24.02.09 Task Group Meeting, Norfolk, VA, Mar. 1977.
- 20 Barsom, J. M., and Rolfe, S. T., "Correlations Between  $K_{Ic}$  and Charpy-V-Notch Test Results in the Transition-Temperature Range," in *Impact Testing of Metals*, ASTM STP 466, ASTM, 1970, pp. 281-302.
- 21 Rolfe, S. T., and Novak, S. R., "Slow-Bend  $K_{Ic}$  Testing of Medium-Strength High-Toughness Steels" in *Review of Developments in Plain Strain Fracture-Toughness Testing*, ASTM STP 463, ASTM, 1970, pp. 124-159.
- 22 Paris, P. C., Tada, H., Zahoor, A., and Ernst, H., "The Theory of Instability of the Tearing Mode of Elastic-Plastic Crack Growth," in *Elastic-Plastic Fracture*, ASTM STP 668, ASTM, 1979, pp. 5-36.
- 23 "EPRI Ductile Fracture Research Review Document," prepared by Marston, T., NP-701-SR, Feb. 1978, EPRI, Palo Alto, Calif.
- 24 Heiser, F. A., "Anisotropy of Fatigue Crack Propagation in Hot Rolled Banded Steel Plate," Lehigh University PhD thesis, Aug. 17, 1969.
- 25 Hertzberg, R. W., and Goodenow, R. H., "Fracture Toughness and Fatigue Crack Propagation in Hot-Rolled Microalloyed Steel," presented at Microalloying 75 Conference, Session 3, p. 8, Oct. 2, 1975, Washington, D.C.
- 26 Wilson, A. D., "Application of the SEM to the Investigation of Inclusion Behavior in Steels," *Scanning Electron Microscopy/1977*, Vol. 1, IIT Research Institute, Chicago, Mar. 1977, pp. 121-128.
- 27 Forsyth, P. J. E., *The Physical Basis of Metal Fatigue*, p. 143, American Elsevier Publishing Company, New York, 1969.
- 28 Pelloux, R. M. N., "Fractographic Analysis of the Influence of Constituent Particles on Fatigue Crack Propagation in Aluminum Alloys," *Transactions of the ASM*, Vol. 57, 1964, p. 511.
- 29 Broek, D., "The Effect of Intermetallic Particles on Fatigue Crack Propagation in Aluminum Alloys," *Fracture*, 1969, Chapman and Hall, London, 1969, p. 754.
- 30 Shih, T., and Araki, T., "The Effects of Non-Metallic Inclusions and Microstructures on the Fatigue Crack Initiation and Propagation in High Strength Carbon Steels," *Transactions of the Iron and Steel Institute of Japan*, Vol. 13, 1973, p. 11.
- 31 McEvily, A. J., "Effect of Constituent Particles on the Notch-Sensitivity and Fatigue Crack Propagation Characteristics in Al-Zn-Mg Alloys," NASA, TID D328, Apr. 1962.
- 32 Hartt, W. H., Fluet, J. E., and Heuke, T. E., "Air Fatigue of Notched 1018 Steel in the Endurance Limit Range," *Metallurgical Transactions*, Vol. 7A, Sept. 1976, pp. 1341-1345.
- 33 El-Soudani, S. M., and Pelloux, R. M., "Influence of Inclusion Content on Fatigue Crack Propagation in Aluminum Alloys," *Metallurgical Transactions*, Vol. 4, Feb. 1973, p. 519.
- 34 Barsom, J. M., "Fatigue-Crack Propagation in Steels of Various Yield Strengths," *ASME Journal of Engineering for Industry*, Vol. 93, Series B, No. 4, Nov. 1971.
- 35 Sullivan, A. M., and Crooker, T. W., "The Effect of Specimen Thickness Upon the Fatigue Crack Growth Rate of A516-60 Pressure Vessel Steel," *ASME Journal of Pressure Vessel Technology*, Vol. 99, No. 2, May, 1977.